ELSEVIER

NeuroImage

www.elsevier.com/locate/ynimg
NeuroImage 38 (2007) 696–707

fMRI during natural sleep as a method to study brain function during early childhood

Elizabeth Redcay,[a,*] Daniel P. Kennedy,[b] and Eric Courchesne[b,c]

[a] *Department of Psychology, University of California, San Diego, La Jolla, CA 92037, USA*
[b] *Department of Neurosciences, University of California, San Diego, La Jolla, CA 92037, USA*
[c] *Center for Autism Research, Rady Children's Hospital San Diego, San Diego, CA 92123, USA*

Received 23 March 2007; revised 30 July 2007; accepted 2 August 2007
Available online 17 August 2007

Many techniques to study early functional brain development lack the whole-brain spatial resolution that is available with fMRI. We utilized a relatively novel method in which fMRI data were collected from children during natural sleep. Stimulus-evoked responses to auditory and visual stimuli as well as stimulus-independent functional networks were examined in typically developing 2–4-year-old children. Reliable fMRI data were collected from 13 children during presentation of auditory stimuli (tones, vocal sounds, and nonvocal sounds) in a block design. Twelve children were presented with visual flashing lights at 2.5 Hz. When analyses combined all three types of auditory stimulus conditions as compared to rest, activation included bilateral superior temporal gyri/sulci (STG/S) and right cerebellum. Direct comparisons between conditions revealed significantly greater responses to nonvocal sounds and tones than to vocal sounds in a number of brain regions including superior temporal gyrus/sulcus, medial frontal cortex and right lateral cerebellum. The response to visual stimuli was localized to occipital cortex. Furthermore, stimulus-independent functional connectivity MRI analyses (fcMRI) revealed functional connectivity between STG and other temporal regions (including contralateral STG) and medial and lateral prefrontal regions. Functional connectivity with an occipital seed was localized to occipital and parietal cortex. In sum, 2–4 year olds showed a differential fMRI response both between stimulus modalities and between stimuli in the auditory modality. Furthermore, superior temporal regions showed functional connectivity with numerous higher-order regions during sleep. We conclude that the use of sleep fMRI may be a valuable tool for examining functional brain organization in young children.
© 2007 Elsevier Inc. All rights reserved.

Keywords: Auditory; Visual; Functional connectivity; Sounds

Introduction

The transition from infancy to the preschool years is a time of dramatic and dynamic neural and cognitive development. For example, brain volume shows a 4-fold increase between birth and about 4 years of age (Courchesne et al., 2000). Synapse density in middle frontal gyrus increases nearly 70% between birth and 4 years of life when it reaches its peak (Huttenlocher and Dabholkar, 1997). Dendritic arbors in frontal cortex grow from 3–11% of adult length at birth to 50% of adult length by age 2 years while arbors in visual cortex reach adult length by age 2 (Huttenlocher, 2002). Cognitive growth during this time is also rapid. For example, children progress from only a few words in their expressive vocabulary at 1 year to full sentences by 3 years of age.

Such dramatic anatomical and behavioral changes must be reflected in changes in brain function during this time. In fact, event-related potential (ERP) studies reveal electrophysiological changes from infancy to the preschool years underlying behaviors such as face processing (e.g., Carver et al., 2003) and language (review: Friederici, 2006). However, electrophysiological methods lack detailed anatomical information. Blood Oxygenated Level Dependent (BOLD) fMRI is a non-invasive tool used to pinpoint the specific brain regions underlying cognitive, social, and perceptual processes. Few studies have directly examined brain function in infants and young children with fMRI due to the difficulty in acquiring such data without motion artifact. For this reason, our knowledge of the functional brain changes seen in the early years of life relies primarily on measures with relatively poor spatial localization capabilities such as ERP, lesion, or anatomy–behavior correlation studies. In order to obtain reliable fMRI data in infants and children, a few studies have been conducted while children were sedated (visual: Born et al., 1996; Martin et al., 1999; Morita et al., 2000; Yamada et al., 2000; Sie et al., 2001; Marcar et al., 2004; auditory and visual: Souweidane et al., 1999; Altman and Bernal, 2001). Sedation is not ethical for use with healthy, typically developing children and thus, these past studies involved children who were clinical patients sus-

* Corresponding author. 8110 La Jolla Shores Dr., Suite 201, La Jolla, CA 92037, USA. Fax: +1 858 551 7931.
E-mail address: eredcay@ucsd.edu (E. Redcay).
Available online on ScienceDirect (www.sciencedirect.com).

1053-8119/$ - see front matter © 2007 Elsevier Inc. All rights reserved.
doi:10.1016/j.neuroimage.2007.08.005

pected of having brain pathology but with negative findings on clinical MRI. Such a sample may still include children with brain abnormalities (e.g., seizures, etc.), since structural MRI is only sensitive enough to detect gross anatomical brain abnormalities. An alternative is to acquire functional MRI data from children during natural sleep. This non-invasive method allows for the acquisition of fMRI data from healthy, typical volunteers recruited from the community.

Two groups have previously examined BOLD fMRI response to auditory stimulation during sleep in infants (Anderson et al., 2001; Dehaene-Lambertz et al., 2002). In the Anderson et al. (2001) study, BOLD activity was detected in response to tones as compared to rest within superior temporal regions in 14 of 20 neonates. Of those 14 neonates, 9 showed BOLD signal decreases during tone presentation. In the study by Dehaene-Lambertz et al. (2002) twenty 2–3-month-old infants were placed in the scanner awake. During fMRI acquisition, 5 were judged to be completely asleep based on behavior, 9 showed ambiguous levels of wakefulness, and 6 were awake. They found bilateral superior temporal activation to both forward and backward speech and a greater response to forward than backward speech in left angular gyrus. A third group has recorded fMRI data from a 6-year-old boy who fell asleep during a language mapping study (Wilke et al., 2003). The authors report strikingly similar patterns of activation in bilateral superior temporal lobes during both sleep and wake states.

A number of basic questions remain regarding the utility of the sleep fMRI technique in early childhood. First, to what degree is BOLD activity differentially modulated by external stimuli during sleep? The Anderson et al. study only presented one auditory stimulus type and the Dehane-Lambertz et al. study contained a majority of infants who were awake for at least portions of the experiment. In the current study, we examined whether presentation of auditory and visual stimuli to 2–4 year olds would produce a differential BOLD response both across and within sensory modalities during sleep. We predicted that stimulus-evoked BOLD response to auditory and visual stimuli would be seen within separable auditory and visual regions, respectively, and furthermore, that the BOLD response within the auditory modality would vary by auditory stimulus type.

A second question is whether stimulus-independent functional networks can be examined in the sleeping young child. To address this question, we utilized a technique called functional connectivity MRI (fcMRI) to reveal the temporal correlation of spontaneous low frequency oscillations across brain regions. The use of fcMRI during rest has revealed correlated stimulus-independent activity within sensory systems including sensorimotor, auditory, and visual regions (Biswal et al., 1995; Cordes et al., 2000; Nir et al., 2006) and also within higher-order associative regions including prefrontal and parietal regions (Greicius et al., 2003; Fox et al., 2005, 2006; Fransson, 2005; Vincent et al., 2006; Seeley et al., 2007). Examination of these networks with fcMRI during wakeful and sleeping adults shows similar functional network maps across states suggesting the examination of stimulus-independent fcMRI is relatively state-independent (Fukunaga et al., 2006). In the current study, we performed a functional connectivity analysis to determine whether stimulus-independent functional networks could be identified during sleep in children. We predicted stimulus-independent functional connectivity patterns would be similar to stimulus-evoked patterns of activation.

Methods

Participants

Functional imaging data were collected from a total of 21 children (7F, 14M) with no known neurological or psychological disorders. Six of the 21 children were presented with visual stimuli only. Nine of the 21 children were presented with auditory stimuli only. Six of the 21 children were presented with both types of experiments (separately) This resulted in a total of 12 successful scan acquisitions for the visual experiment (mean age = 46.4 ± 6.7 months) and 15 successful scan acquisitions for auditory experiments (mean age = 46.9 ± 9.7 months). Two of the 15 scans from auditory experiments were excluded due to excessive motion artifacts (see criterion below) (see Table 1 for participant information). All children were recruited from magazines and flyers in the community as part of an on-going longitudinal structural MRI study in our laboratory. The Institutional Review Board of Children's Hospital and the University of California, San Diego approved this study. Parents of the participants gave informed written consent for their child to participate in this study and were compensated monetarily for their time. Hearing was reported by parents as normal for all participants on which a Family Medical History questionnaire was obtained. This form was

Table 1
Participants information for auditory and visual experiments

Subject	Experiment	Age (months)	Sex	Cognitive score (mean 100)
S1	A	30.51	F	94
S2	A	33.99	M	121
S3	A	51.35	M	115
S4	A	53.52	F	124[a]
S5	A	57.30	F	108
S6	A	57.93	M	111
S7	A	36.92	M	82[b]
S8	A,V	39.58	F	138
S9	A,V	40.67	M	99
S10	A,V	46.62	M	124[a]
S11	A,V	47.28	M	122
S12	A,V	55.66	M	110*
S13	A,V	57.99	F	109*
S14	V	36.39	M	123
S15	V	36.72	M	118
S16	V	38.83	F	90
S17	V	41.36	M	131
S18	V	44.75	F	134[c]
S19	V	50.76	M	141
Auditory	$n=13$	46.87 (9.66)	8M5F	114 (17.78)
Visual	$n=12$	44.72 (7.16)	8M4F	122 (16.38)

'A' refers to the auditory experiment; 'V' refers the visual experiment. Unless otherwise noted, cognitive score refers to the Composite score from the Mullen Scales of Early Learning.

* Denotes participants whose date of cognitive testing was greater than 2 months from scan acquisition

[a] Denotes Full Scale IQ from the Weschler Intelligence Test.

[b] Denotes a score taken from a child who was non-compliant at time of testing. Follow-up testing 6 months later revealed a Composite Score within normal range.

[c] Denotes General Conceptual Ability from the Different Abilities Test.

Means (standard deviations) for the auditory and visual experiment are given at the bottom of the table.

not collected for five individuals; however no hearing deficits were observed in these individuals.

Auditory experiments

For auditory experiments ($n=13$), children were presented with four 20-s blocks of each condition: vocal sounds (V), nonvocal sounds (NV), and tones (T). Each auditory condition was separated by a 15-s "rest" condition in which no stimulus was presented. Four of the 13 children were presented with a slightly different design in which an additional block of speech stimuli was included (although not analyzed here) and each condition was separated by an alternating 5- or 15-s rest period. Each experimental block was 20 s and was repeated 4 times like the other auditory design. Experiments were presented in a semi-counterbalanced block design to maximize power to detect signal changes. For further design details see supplementary information Fig. S1. The vocal and nonvocal sounds in this study were taken from previous studies of environmental sound processing by Saygin and colleagues (Saygin et al., 2003, 2005; Cummings et al., 2006). Vocal sounds included only human vocal sounds (e.g., a cough, sneeze, or a baby's cry). Nonvocal sounds included both environmental sounds and non-human vocal sounds (e.g., a hammer drilling, a train, and a dog barking). These sounds were taken from the Digifex and BBC digital sound effect libraries. The sampling rate was 44.1 kHz at 16-bit resolution. The tone stimuli were created using Cool Edit 2000 digital audio software (Syntrillium Software Corp., Scottsdale, AZ). Three different complex tones were created by using varying base frequencies (220, 660, 990 Hz) to create chord stimuli. All sounds were normalized for intensity. However, the sounds utilized were naturalistic and consequently, each vocal sound contained slightly greater periods of lower amplitude sound than most of the nonvocal sounds (e.g., a natural laugh vs. a continuous train). Mean amplitudes across each 20-s block period were comparable, but reduced by 6 dB in the vocal sounds condition (vocal 73.5 dB; non-vocal 79.5 dB; tones 78.6 dB). The stimuli were presented from a stereo to the subject via a MRI-compatible pneumatic headphone system.

Visual experiment

For the visual experiment ($n=12$), children were presented with 8 repetitions of 20-s blocks of flashing lights at 2.5 Hz separated by 20 s during which time no stimulus was presented. Stimuli were programmed using Presentation software (www.neurobs.com) and presented through a PC laptop and projector.

Procedure

All children were imaged during natural sleep without the use of sedation. Prior to the night of scanning, families were asked to play CDs with the sounds of the MRI scanner and practice inserting earplugs into the child's ears while he or she fell asleep at home. Parents and children arrived at the scanner between 9:00 and 10:00 PM. The child was allowed to fall asleep naturally either in the waiting room or the scanner room. After 5–10 min of sleep on the scanner bed, earplugs and headphones were placed on the child. Earplugs were used to filter out background scanner noise and reduce startle responses with the onset of speech sounds. The child's parent and a researcher remained in the scanner room during the entire scan session. A mirror was placed over the head coil to allow the researcher to observe the child during scanning. If the child awoke, data acquisition was immediately halted and the child was removed from the scanner.

Functional imaging acquisition

Images were acquired on a Siemens Symphony 1.5 Tesla Scanner at the UC San Diego Hillcrest Medical Center. Whole brain axial slices were collected with a gradient-recalled echo-planar imaging (EPI) pulse sequence (TR (repetition time)=2500 ms; flip angle=90°; field of view (FOV)=256 mm; matrix=64×64 (4 mm by 4 mm in-plane resolution); slice thickness=4 mm; # of slices=30; # of volumes for auditory=172 or 198; # of volumes for visual=134). A T1-weighted anatomical image using an MPRAGE sequence was collected during each scan session for co-registration with the functional images. Anatomical scans were collected in the coronal plane (FOV=256 mm; matrix=256×256; slice thickness=1.5 mm; # of slices=128).

Individual data analyses

All fMRI analyses were conducted with the Analysis of Functional NeuroImages statistical software package (AFNI (version 5-31-2006); http://afni.nimh.nih.gov/afni; Cox, 1996). Motion correction and three-dimensional registration of each participant's functional images were performed using an automated alignment program (3dvolreg), which co-registered each volume in the time series to the middle volume acquired in that run using an iterative process. The output translational and rotational parameters from the motion alignment program were examined to determine the amount of motion during the scan. For all of the participants included, time points in which the sum of the root mean square of the rotational and translational parameters was greater than 0.4 were not included in the analysis. For the auditory experiments, 4 individuals had time points removed from the analysis (average percent of run=5.0±3.3%). For the visual experiment, 4 individuals had time points removed from the analysis (average percent of run=4.4±2.1%). If greater than 10% of the functional run contained a summed motion value greater than 0.4, the subject was not included in the analysis. Two of 15 scans acquired for the auditory experiment did not pass this motion criterion and so were not included in the analysis. Additionally, the first two volumes in each data series were not included in order to exclude noise due to T1 equilibration effects. Images were smoothed with a Gaussian filter (full-width half-maximum=6 mm).

FMRI data were normalized to percent signal change from baseline (i.e., "rest" periods during which no stimuli were presented). Specifically, the mean MR signal value from baseline at each voxel was subtracted from the MR signal value at each time point in the series on a voxel-by-voxel basis. The resulting value was then divided by the mean MR signal value from baseline for that voxel and multiplied by 100. The mean baseline value did not include time points that had been removed from the analysis due to motion.

Individual multiple linear regression analyses of percent signal change values were conducted. For the auditory experiment, 9 input stimulus functions were modeled; 1 of vocal sounds; 1 of nonvocal sounds, 1 of tones, and 6 translational and rotational motion parameters. For the visual experiment, 7 input stimulus functions were modeled; 1 for the flashing light condition, and 6 translational and rotational parameters. The regression included

terms to remove both the linear trend and the global mean. In this method, an impulse response function (IRF) is first estimated from the input stimulus function and the time series data. This IRF is then convolved with the time series data to determine a goodness of fit (or linear contrast weight). Each linear contrast weight was modeled between 0, 2.5, 5, and 7.5 s.

Group fMRI analyses

Data were registered into standard space based on the Talairach atlas (Talairach and Tournoux, 1988). Although the Talairach template is based on an adult, studies from our lab have revealed comparable anatomical co-registration among groups of 1–2 year olds, 3 year olds, and adults (Redcay et al., in press, Supplementary Information). However, while the use of the Talairach template produces good co-registration within very young children in a narrow age range, the Talairach coordinates do not necessarily correspond to the same areas of activation. For this reason, regions of activation were identified based on anatomical landmarks, rather than coordinates. The Talairach coordinates are given in Tables 2, 3, and 4 for reference; however the reader should use caution when extrapolating these to the adult brain. For the auditory experiment, a 1-way repeated measures ANOVA was run with condition (V, NV, T) as the repeated measure. Whole brain contrasts were run between each condition to determine which brain areas showed a differential response to the different types of auditory stimulation. A contrast of "All" stimuli was modeled in order to determine the regions responsive to all three auditory stimulus types. For the visual experiment, a two-tailed, unpaired *t*-test was conducted comparing percent signal change during the flashing light condition as compared to 0. For both experiments, group maps were created at an intensity threshold of $p<0.005$ and a minimum cluster size of 740 mm^3. This cluster volume was determined using an iterative Monte Carlo simulation to determine the minimum cluster size needed to protect a whole brain voxel-wise alpha of $p<0.05$.

Table 2
Regions within auditory and visual ROA masks

Region	Hemi	BA	*x*, *y*, *z*	*t*-value
Auditory: All sounds vs. rest				
Left STG cluster				
Superior temporal gyrus	L	42	(58, 26, 10)	6.34
Superior temporal gyrus	L	41	(42, 26, 7)	5.85
Superior temporal gyrus	L	22	(50, 34, 7)	4.52
Right STG cluster				
Superior temporal gyrus	R	22	(−54, 6, −5)	6.27
Superior temporal gyrus	R	22	(−47, 21, 7)	5.27
Superior temporal gyrus	R	22	(−54, 15, 3)	5.23
Supramarginal gyrus	R	40	(−51, 33, 22)	3.81
Left lingual gyrus cluster				
Lingual Gyrus	L	18	(6, 73, −10)	5.48
Right Cerebellum cluster				
Cerebellar Hemisphere	R		(−19, 61, −22)	5.72
Visual: Flashing lights vs. rest				
Bilateral visual cortex cluster				
Cuneus	R	30	(−3, 69, 8)	8.71
Cuneus	L	30	(3, 69, 8)	8.01
Lingual gyrus	B	18	(0, 81, −3)	8.20
Superior occipital gyrus	L	19	(1, 77, 28)	6.59

Four clusters were identified in the All sounds vs. rest comparison.
One cluster was identified in the Flashing lights vs. rest comparison.
For each cluster, Talairach coordinates for the voxels with the peak *t*-value for each region within that cluster are given.
Hemi designates the hemisphere active: left (L), right (R), or bilateral (B).

For auditory and visual experiments, Regions of Activation (ROAs) were identified based on group analyses. Specifically, for the auditory experiment, the ROAs were created from the activation map for the contrast of "All" auditory stimuli as compared to rest. For the visual experiment, the ROA was created from the activation map for flashing lights as compared to rest. Signal timecourses were extracted from these ROAs from each individual and used in the stimulus-evoked analyses and the functional connectivity analyses as described below.

Mean percent signal change for each individual was extracted from within each of these group-defined ROAs and averaged over each of the block presentations. For the auditory experiment, percent signal for each block was plotted separately for each condition and each ROA. To determine whether the sleeping brain differentiates between auditory stimulus types, percent signal change values from the 3 auditory conditions (V, NV, T) were averaged over the first 5 to 17.5 s of each block. A repeated-measures ANOVA was run using SPSS (www.spss.com/spss) first on these averaged percent signal values to determine if there was a main effect of condition. Next, repeated-measures ANOVAs were run at each time point for each ROA to determine when a main effect of condition was seen during each block.

Functional connectivity analyses

Several additional pre-processing steps were included for the fcMRI analyses. The functional volumes were temporally bandpass filtered ($0.01<f<0.1$) before conversion to percent signal change. Next, multiple linear regression analysis was used to model several types of noise in the functional data, which were then removed as regressors of no interest: the linear trend, the global signal (average intensity of every voxel across the entire brain calculated for each time point), 6 motion parameters (3 rotational and 3 translational directions) and their 6 temporal derivatives. The resulting pre-processed functional data were then registered into Talairach space.

We utilized a seed-based method so that regions of activation (ROA) identified in the stimulus-evoked analyses could be used as seed regions in the functional connectivity analyses. An alternative method to perform functional connectivity analyses is to use spatial ICA (for a discussion of strengths and weaknesses of both methods see Bartles and Zeki, 2005). For each region of activation and each individual subject, the average regional timecourse was extracted and then used to calculate a correlation coefficient between that particular region and all other voxels in the brain.

As the purpose of this analysis was to determine whether *stimulus-independent* functional connectivity analyses might reveal functional networks in sleeping children, we examined occipital cortex connectivity using the auditory dataset, and the superior temporal cortex connectivity using the visual dataset. Since the functional activation to the auditory and visual stimuli showed only minimal overlap (see Results) the functional connectivity results can be thought to be independent of the stimuli presented during the data acquisition. While this approach approximates stimulus-independent datasets, it is not ideal, as other stimuli are present during data acquisition. For example, scanner noise is constant throughout the entire experiment. Caveats aside, for the remainder of this paper, we refer to this analysis as stimulus-independent functional connectivity.

Seed regions were defined based on the results of the stimulus-evoked auditory and visual experiments. Specifically, the two largest functionally-defined regions of activation (ROAs) from the auditory experiment during the "All" condition vs. rest (intensity threshold $p<0.001$, corrected) served as auditory seed regions. Similarly, the largest functionally-defined region of activation from the visual experiment (intensity threshold $p<0.0001$) served as the visual seed region. We chose different intensity thresholds so that

Table 3
Regions responsive to auditory conditions

Region	Side	BA	*x*, *y*, *z*	*t*-value
Condition vs. rest				
Vocal sounds				
Vocal>rest				
Superior temporal gyrus	R	22	(−54, 24, 7)	3.92
Rest>Vocal				
Medial superior frontal gyrus	B	6	(2, −10, 46)	−4.63
Precental gyrus	R	4	(−29, 20, 47)	−4.65
Posterior cingulate gyrus	R	31	(−10, 37, 32)	−4.34
Thalamus	R		(−5, 17, 10)	−4.72
Nonvocal sounds				
Nonvocal>rest				
Cortical				
Medial frontal gyrus	B	32/10	(−2, −51, 2)	5.31
Transverse temporal gyrus	L	41	(39, 17, 6)	4.42
Superior temporal gyrus	R	22	(−53, 4, −1)	8.95
Superior temporal gyrus	L	22	(55, 18, 8)	6.87
Superior temporal sulcus	R	21/22	(−58, 33, −1)	5.08
Cingulate gyrus	L	31	(13, 21, 31)	4.79
Cuneus	L	19	(2, 89, 27)	4.89
Lingual gyrus	L	19	(19, 73, 2)	3.99
Subcortical				
Cerebellum	L		(35, 64, −33)	6.14
Cerebellum	R		(−18, 64, −24)	5.76
Rest>Nonvocal				
None				
Tones				
Tones>rest				
Cortical				
Anterior cingulate	L	24	(6, −40, 2)	5.30
Medial frontal gyrus	B	32	(3, −39, 10)	5.82
Medial frontal gyrus	R	9	(−13, −34, 31)	5.12
Superior temporal gyrus	R	22	(−54, 18, −1)	6.62
Superior temporal gyrus	L	22	(62, 26, 11)	6.61
Superior temporal sulcus	R	22	(−49, 37, 6)	4.74
Middle temporal gyrus	R	37	(−37, 59, 2)	6.20
Middle temporal gyrus	L	22	(54, 37, 2)	5.90
Lingual gyrus	L	19	(11, 65, −2)	4.54
Cuneus	L	31	(14, 66, 10)	4.16
Insula	R		(−31, −10, 1)	4.92
Subcortical				
Putamen	R		(−19, −15, −8)	6.72
Putamen	L		(17, −15, −2)	5.12
Cerebellum	L		(31, 68, −25)	4.98
Cerebellum	R		(−34, 62, −38)	4.81
Rest>Tones				
None				
Nonvocal>Vocal				
Cortical				
Anterior cingulate	B	24	(3, −31, −9)	4.52
Medial frontal cortex	B	10	(3, −57, 2)	5.73
Medial frontal cortex	B	32	(5, −47, 15)	5.09
Medial superior frontal gyrus	L	6	(5, −14, 51)	5.88
Precentral gyrus	L	4	(30, 15, 36)	6.42
Precentral gyrus	R	4	(−46, 10, 43)	6.36
Superior temporal gyrus	R	22	(−54, 12, 7)	3.95
Superior temporal sulcus	R	21/22	(−50, 13, −7)	4.44
Cingulate gyrus	L	31	(5, 18, 26)	6.06
Lingual gyrus	R	17	(−17, 89, 1)	5.07
Lingual gyrus	L	17	(16, 89, −6)	4.01
Subcortical				
Parahippocampal gyrus	R		(−18, 17, −21)	5.51
Parahippocampal gyrus	L		(22, 20, −22)	4.93
Cerebellum	R		(−34, 54, −24)	6.71
Cerebellum	L		(18, 44, 21)	6.26
Tones>Vocal				
Cortical				
Anterior cingulate	B	24	(−2, −31, −10)	5.56
Medial frontal cortex	R	32/10	(−9, −50, 11)	7.13
Medial frontal cortex	L	10	(6, −50, 19)	6.15
Medial superior frontal gyrus	L	6	(5, −14, 46)	4.20
Superior frontal gyrus	R	9	(−25, −42, 14)	5.74
Superior frontal gyrus	L	9	(17, −42, 16)	5.01
Superior frontal gyrus	R	6	(−14, −15, 51)	4.49
Middle frontal gyrus	R	9	(−41, −23, 19)	5.38
Inferior frontal gyrus	L	9	(39, −3, 23)	5.36
Inferior frontal gyrus	R	47	(−41, −18, −2)	3.99
Superior temporal gyrus	R	22	(−50, 9, −2)	7.21
Precentral gyrus	R	4	(−45, 5, 35)	5.41
Precentral gyrus	L	4	(43, 9, 31)	5.04
Posterior cingulate	B	31	(6, 42, 30)	5.11
Precuneus	R	7	(−14, 53, 43)	4.88
Inferior parietal lobule	R	40	(−49, 33, 34)	4.73
Superior parietal lobule	L	7	(33, 70, 43)	4.50
Supramarginal gyrus	L	39	(42, 54, 31)	3.76
Subcortical				
Cerebellum	L		(25, 64, −34)	7.72
Cerebellum	R		(−18, 74, −32)	6.19
Nonvocal>Tones				
None				

Hemi designates hemisphere active: left (L), right (R), bilateral (B). Talairach coordinates are given for the peak *t*-value within each region or Brodmann Area.
Regions of greater activation to rest as compared to an auditory condition were seen in the vocal sounds condition only.

the seed regions were roughly similar in size (left STG: 100 voxels; right STG: 139 voxels; occipital cortex: 171 voxels).

For group analyses, individual correlation coefficient maps derived from each seed region were normalized using Fisher's *r*-to-*z*′ transformation. Next, two separate two-tailed unpaired *t*-tests were run, which resulted in the *z*′ functional maps. These maps were thresholded at an intensity of $p<0.005$, and cluster corrected at a spatial threshold of 740 mm^3, as described in the fMRI group analyses.

Results

Differential response to auditory and visual stimuli

A one-way repeated measures ANOVA revealed regions significantly responsive to all auditory stimuli (NV, V, T) as compared to no auditory presentation ($p<0.005$, corrected). These regions included bilateral superior temporal gyri and sulci, left lingual gyrus, and right lateral cerebellum (Table 2; Fig. 1). These regions comprised the four auditory ROAs.

Visual flashing lights, on the other hand, elicited significant BOLD response localized to parietal and occipital regions (Fig. 2; Table 2). Specifically, *t*-test analyses revealed a BOLD signal decrease in response to visual flashing lights as compared to no flashing light presentation localized to bilateral medial cuneus, bilateral lingual gyrus, and superior occipital gyrus. These regions comprised the visual ROA. It is not clear from the current study whether the negative *t*-values in occipital cortex reflect a decrease in BOLD signal from 'rest' or a negative BOLD response. Throughout the paper we refer to the negative *t*-values in the visual cortex as a 'BOLD signal decrease'.

Overlay of the visual and auditory activation maps revealed a small region of overlap only within left lingual gyrus. This functional region of 16 voxels was 1.9% and 6.9% of the total number of voxels active for the visual and auditory experiments, respectively.

Differential response within auditory modality

Both whole-brain and ROA analyses were used to determine whether a differential response to the 3 types of auditory stimuli was seen. In the whole-brain analyses, each auditory condition elicited activation in the right superior temporal gyrus ($p<.005$, corrected). However, nonvocal sounds and tones additionally elicited activation in a broad number of other regions including left STG, right STS, medial frontal cortex, left lingual gyrus, left cuneus, and bilateral cerebellum (Fig. 3; Table 3). Direct comparison of vocal versus nonvocal sounds revealed greater activation to the nonvocal sounds within a number of regions including medial frontal cortex (including anterior cingulate cortex), right STG/S, bilateral lingual gyrus, and bilateral cerebellum (see Table 3 for complete list). Similarly, direct comparison of vocal sounds versus tones revealed greater activation to tones within a number of regions including medial prefrontal cortex (including anterior cingulate cortex), bilateral cerebellum, and right STG (Table 3 for complete list). Interestingly, activation maps to nonvocal sounds and tones did not significantly differ from each other.

For the ROA analyses, a repeated-measures ANOVA was run for each of the 4 ROAs. The repeated measure was the mean value within the ROA for each condition (V, NV, T). A main effect of condition was seen in the left superior temporal gyrus ($F(2,11)=3.697$; $p<0.04$) and right cerebellum ($F(2,11)=3.620$; $p<0.042$). Additionally, a repeated-measures ANOVA from each time point across the period of sound presentation revealed a main effect of condition type (V, NV, T) at time point 5 (10 s into the block) for the left STG ($F(2,11)=6.391$; $p<0.006$) and time point 6 (12.5 s into the block) for the left ($F(2,11)=4.609$; $p<0.02$) and right STG ($F(2,11)=6.391$; $p<0.045$). A main effect of condition was seen in the right cerebellum at time point 1 (the start of the stimulus presentation) ($F(2,11)=4.927$; $p<0.016$) and time point 7 (15 s into the block) (Fig. 1).

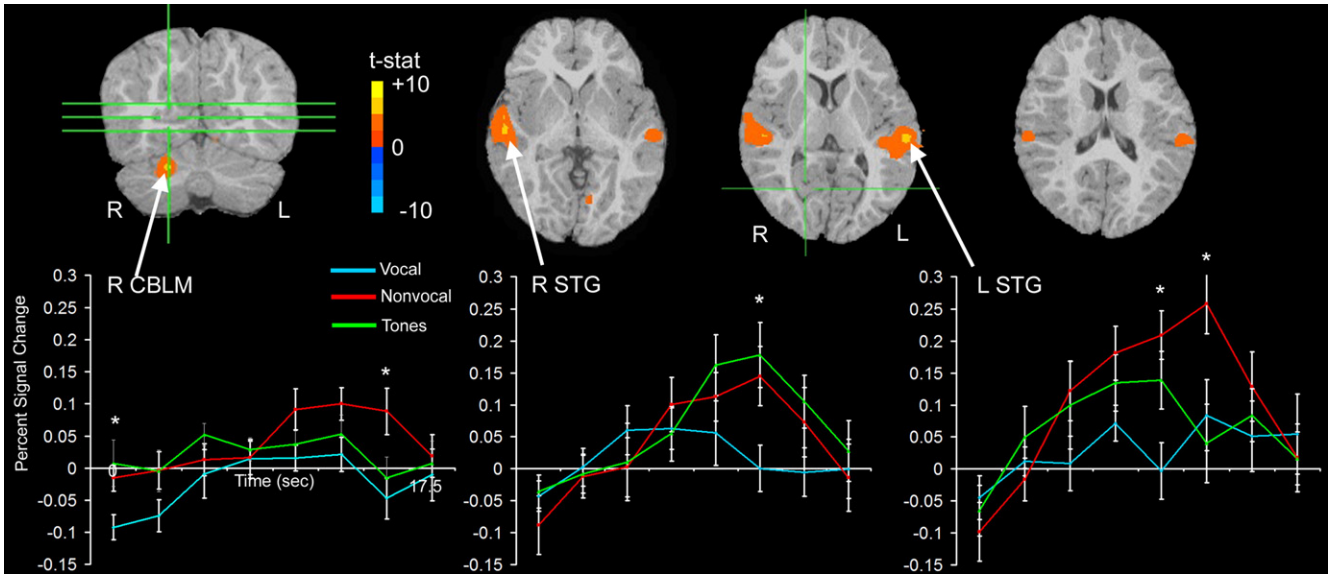

Fig. 1. Group functional activation to All sounds combined vs. rest. The map of functional activation to All sounds combined is displayed on images from a single representative subject ($p<0.005$, corrected). Mean percent signal change values from 3 ROAs identified in the All sounds contrast, right cerebellar hemisphere (R CBLM), right superior temporal gyrus (R STG), and left superior temporal gyrus (L STG), were extracted from each individual. Percent signal change for each condition (averaged across each repetition) is plotted by time (s). Statistically significant differences between conditions are noted by an '*' at different time points in each of the 3 regions of interest.

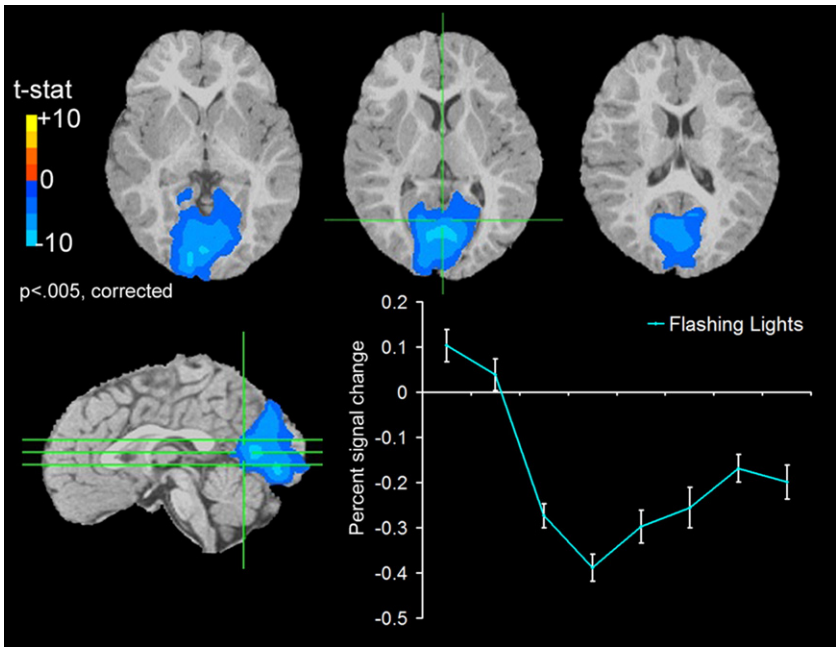

Fig. 2. Group functional activation to flashing lights vs. rest. Presentation of flashing lights at 2.5 Hz produced negative activation patterns in primary visual cortex and surrounding occipital regions. Functional activation maps at $p < .005$, corrected are displayed on images from a single representative subject. Percent signal change values were extracted from within the visual ROA and plotted across time (s).

A motion analysis revealed no significant differences in the total amount of movement between conditions ($F(1,2) = 0.857$; $p < 0.428$) in the auditory experiment.

Functional connectivity

Functional connectivity analysis of the visual dataset, using seed volumes (ROAs) derived from the auditory experiment, identified temporal correlations in BOLD signal in many of the same regions as those seen in the stimulus-evoked auditory experiment. However, the extent and number of brain regions identified in stimulus-independent fcMRI analyses was greater than in the stimulus-evoked conditions as compared to rest (Fig. 4; Table 4). For example, additional regions were found to be strongly correlated with the right STG ROA including bilateral inferior frontal gyri, posterior middle temporal gyri, and fusiform gyri which were not seen in the stimulus-evoked analyses. Similarly, frontal regions including bilateral inferior and left middle frontal gyrus showed a strong correlation with the left STG ROA but were not seen in the stimulus-evoked analyses. Further, the region of medial frontal cortex that was correlated with left STG was more dorsal than that seen in the stimulus-evoked analyses. The only regions identified in the stimulus-evoked analyses which were not seen in the fcMRI analyses were the cerebellum, cuneus/lingual gyrus, and putamen.

In an additional analysis, we examined the functional connectivity of the L and R STG seed region when flipped to the contralateral hemisphere. This was done to examine whether any potential hemispheric differences in connectivity were due to true hemisphere effects or slight differences in the location of the L and R STG seed regions. These data are presented in Supplementary Material (Fig. S2).

Functional connectivity analysis of the auditory dataset using a seed volume (ROA) derived from the visual dataset revealed a different pattern of functional connectivity than that of auditory seed volumes in the visual dataset. The functional connectivity map revealed a peak region of connectivity within primary visual cortex [peak t-value 29.72; Talairach coordinate (−3, 85, 7)], extending into bilateral cuneus, bilateral precuneus, bilateral lingual gyri, and into middle temporal gyrus. Additionally, a cluster of bilateral paracentral lobule [peak t-value = 7.32; Talairach coordinate (−3, 41, 60)] also showed functional connectivity with the occipital seed volume. These regions included the region of stimulus-evoked negative response to visual flashing lights, but, as with the auditory seeds, a greater number of brain regions were identified in the fcMRI analyses.

Discussion

We have provided evidence that reliable fMRI data can be collected from very young children during sleep. We found differential patterns of stimulus-evoked brain activity both within a single stimulus modality (auditory) and across stimulus modalities (auditory and visual). Additionally, we found stimulus-independent patterns of activation that were similar, although greater in extent, to those seen during stimulus-evoked analyses. These findings add to the growing body of literature from electrophysiological and fMRI studies suggesting that the sleeping brain can process and discriminate externally presented stimuli (Perrin et al., 1999; Portas et al., 2000; Bastuji et al., 2002; Cheour et al., 2002a,b; Martynova et al., 2003; Pena et al., 2003; Wilke et al., 2003). Furthermore, through our functional connectivity analyses, we show that intrinsic, coherent, BOLD fluctuations can be examined during sleep. Analyses of these stimulus-independent functional networks could be a valuable tool in examining the emergence and refinement of network activity in typical and atypical development.

A limitation of the current study is that we did not utilize concurrent polysomnographic recording and thus sleep stage could

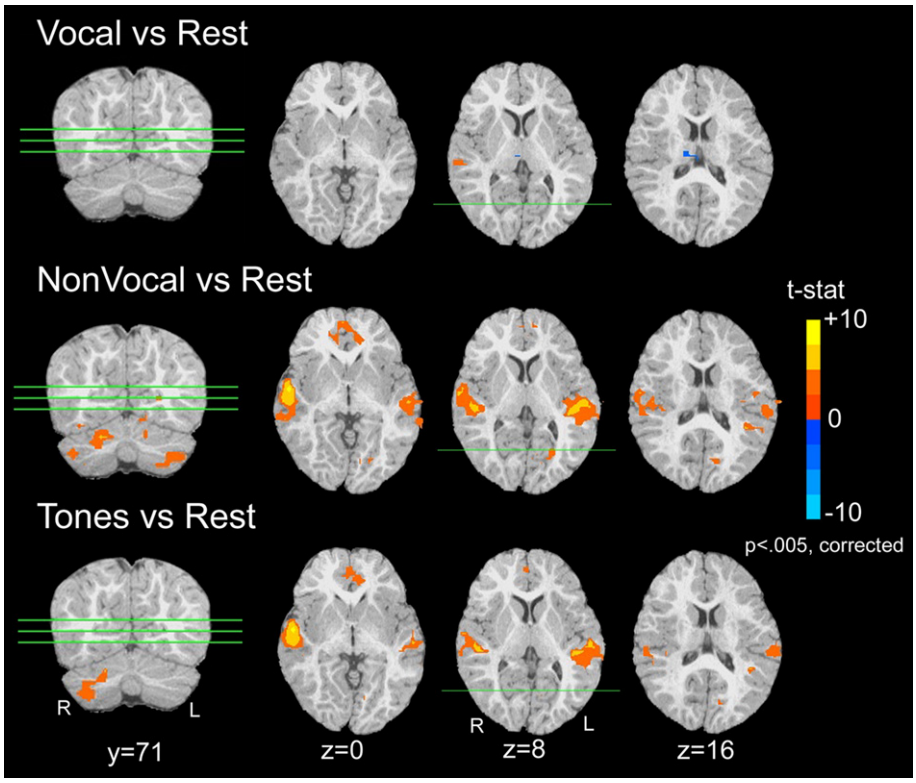

Fig. 3. Group functional activation maps to each auditory condition vs. rest. Functional activation maps at $p<0.005$, corrected are displayed on images from a single representative subject. Maps are given for each of the three auditory conditions vs. rest. The response to nonvocal sounds and tones produced similar patterns of activation including bilateral superior temporal, medial frontal, and cerebellar regions. The response to vocal sounds, however, was restricted to right superior temporal gyrus. Axial coordinates (x,y,z) are given for each slice.

not be definitively identified. However, evidence suggests children in this age range have a mean REM onset latency of 90 min. We collected these data after approximately 40–55 min of sleep and thus can be reasonably confident that a majority of participants were in NREM sleep during data acquisition. Variability in sleep stage could add variability in the functional response across participants; however, we have little reason to expect systematic within-participant differences in sleep stage between conditions as conditions were presented in semi-counterbalanced order. For example, one possibility is that a particular condition could elicit a change in sleep stage as compared to other conditions. A previous study of sleeping adults showed slight differences in alpha power during SII sleep following presentation of their own name, a stimulus of high personal significance, but not other names ($p<0.045$) (Perrin et al., 1999). While we did not record EEG, analyses of movement parameters did not reveal significant differences in movement between conditions, a finding which might be expected if one condition elicited transition to a lighter stage of sleep. Thus, the within-group differences in the response to auditory stimuli were likely not sleep stage dependent. However, further studies utilizing concurrent recording of sleep stages will be useful to verify this claim.

In previous fMRI studies during sleep in infants (Dehaene-Lambertz et al., 2002), children (Wilke et al., 2003) and adults (Portas et al., 2000; Czisch et al., 2002, 2004; Tanaka et al., 2003; Wehrle et al., 2007), the BOLD response showed similarities to wakefulness in some cases but also some differences across a variety of sleep stages and stimulus types. For example, several studies report a reduced extent or intensity of the BOLD signal in auditory cortices in response to a variety of acoustic stimuli during NREM sleep (Tanaka et al., 2003) and during REM sleep without rapid eye movements (Wehrle et al., 2007) while others report no difference in auditory cortices between sleep and wakefulness (Portas et al., 2000; Dehaene-Lambertz et al., 2002; Wilke et al., 2003), and still others report BOLD signal decreases in NREM stage 2 sleep in adults (Czisch et al., 2004). Furthermore, a study of 2–3-month-old infants revealed comparable levels of superior temporal activation during sleep and wakefulness, but a greater response in right dorsolateral prefrontal cortex to speech as compared to non-speech in wakefulness as compared to sleep (Dehaene-Lambertz et al., 2002). In the current study, the BOLD response to all auditory stimuli combined vs. rest was very similar to that which would be expected in studies of the awake older child or adult. Specifically, bilateral superior temporal gyrus/sulcus and right cerebellum were recruited. However, the pattern of discrimination between stimuli differed from that identified in previous studies of the awake state. In fMRI studies of the adult brain, vocal sounds elicit greater activity within bilateral STS and STG in comparison to nonvocal sounds (Belin et al., 2000, 2002). In the current study, we found the opposite effect; namely, nonvocal sounds and tones elicited greater activation in more regions (bilateral STG, medial frontal cortex, and cerebellum) than did vocal sounds.

Future studies are needed to determine why the response to vocal sounds is reduced in temporal, frontal, and cerebellar regions, as compared to nonvocal sounds and tones. One possibility is that the reduced mean dB level within the vocal sounds condition may have contributed to the reduced intensity

Table 4
Auditory regions of functional connectivity in the visual dataset

Seed	Region	Hemi	*x*, *y*, *z*	*t*-value
L STG				
	Medial prefrontal cortex	B	(6, −43, 36)	5.03
	Superior frontal gyrus	R	(−15, −47, 24)	5.32
	Middle frontal gyrus	L	(30, −47, 7)	6.15
	Inferior frontal gyrus	R	(−47, −12, 15)	6.64
	Inferior frontal gyrus	L	(45, −19, 27)	5.89
	Transverse temporal gyrus	L	(45, 28, 12)	12.89
	Transverse temporal gyrus	R	(−42, 17, 12)	10.02
	Superior temporal gyrus	L	(57, 20, 4)	16.15
	Superior temporal gyrus	R	(−54, 16, 7)	10.33
	Posterior middle temporal gyrus	L	(38, 56, 20)	8.24
	Posterior middle temporal gyrus	R	(−43, 56, 15)	7.16
	Inferior postcentral gyrus	L	(58, 21, 15)	15.97
	Precuneus	L	(6, 44, 47)	5.38
	Middle cingulate gyrus	R	(−11, 24, 36)	4.79
	Anterior insula	L	(33, −23, 7)	5.09
	Anterior insula	R	(−30, −23, 3)	4.73
R STG				
	Medial prefrontal cortex	B	(−6, −40, 19)	7.36
	Inferior frontal gyrus	R	(−42, −28, −4)	5.75
	Inferior frontal gyrus	L	(41, −39, 0)	6.87
	Superior temporal gyrus, extending to transverse temporal gyrus	R	(−58, 8, 3)	23.73
	Superior temporal gyrus, extending to transverse temporal gyrus	L	(49, 24, 8)	12.18
	Superior temporal sulcus	R	(−43, 29, 3)	9.61
	Posterior middle temporal gyrus	R	(−51, 53, 0)	4.54
	Posterior middle temporal gyrus	L	(38, 56, 19)	4.75
	Fusiform gyrus	R	(−35, 45, −16)	5.84
	Fusiform gyrus	L	(38, 44, −20)	7.06
	Supramarginal gyrus	R	(−51, 49, 32)	5.95
	Insula	R	(−39, −11, 3)	5.04
	Insula	L	(41, −4, 4)	6.45
	Hippocampus	R	(−19, 12, −16)	5.87

Hemi designates hemisphere active, left (L), right (R), bilateral (B).
Talairach coordinates (*x*,*y*,*z*) are given for the peak *t*-value within each region.

and extent of activation within auditory cortices during vocal sound presentation. In fact, an increase of 10 dB sound level has been shown to result in an increased extent or intensity of activation within auditory cortex (Jancke et al., 1998; Langers et al., 2007). However, in the present study, we found functional differences between conditions not only in auditory cortex, but also in a number of higher-order regions. Given that increases in dB level have only been reported to affect auditory cortical regions, it seems unlikely that differences in mean sound level alone could account for the differences we reported between the vocal and other sound conditions. An alternative explanation is that the neural response to some types of stimuli may actually be altered during sleep as compared to the awake state, a suggestion that is consistent with previous ERP studies (Bastuji et al., 2002; Perrin et al., 2002). In an ERP study in adults, the N400, an ERP component reflecting semantic discordance, was measured in response to congruous, incongruous, and pseudo-words during sleep and awake states. In the awake state, pseudo-words show the greatest N400 response as they are the least semantically related to the probe word; incongruous words show a greater N400 response than congruous words as well but not as large as that of pseudo-words. During sleep stage 2 (NREM) and REM sleep, incongruous words showed a greater response than congruous words; however, during REM sleep, pseudo-words showed a smaller N400 than incongruous words (Perrin et al., 2002). This pattern suggests that a different hierarchical response to some stimuli is present during sleep. Follow-up studies using sound stimuli of identical bandwidth, duty cycle, and intensity would be necessary to verify whether an altered hierarchy of response is present for vocal and nonvocal sounds during sleep.

For the current study, we deemed it infeasible to conduct a sparse sampling technique with children during sleep due to the high probability that the repetitive, abrupt onset of scanner gradient noise could likely startle and wake the children. However, the presence of continuous scanner background noise (SBN) has been shown to confound auditory studies of the awake adult by leading to increased baseline levels and nonlinearity effects in auditory cortices (Gaab et al., 2006). The effect of SBN on auditory processing during sleep has not been directly investigated and some evidence suggests its effect during sleep may be quite different from that of the awake state (Tanaka et al., 2003). Several studies which did *not* use 'silent' imaging techniques reveal robust activation of auditory cortices during sleep (Portas et al., 2000; Dehaene-Lambertz et al., 2002; Wilke et al., 2003). Nonetheless, this potential confound would not be expected to differentially affect one condition over another and thus likely can not account

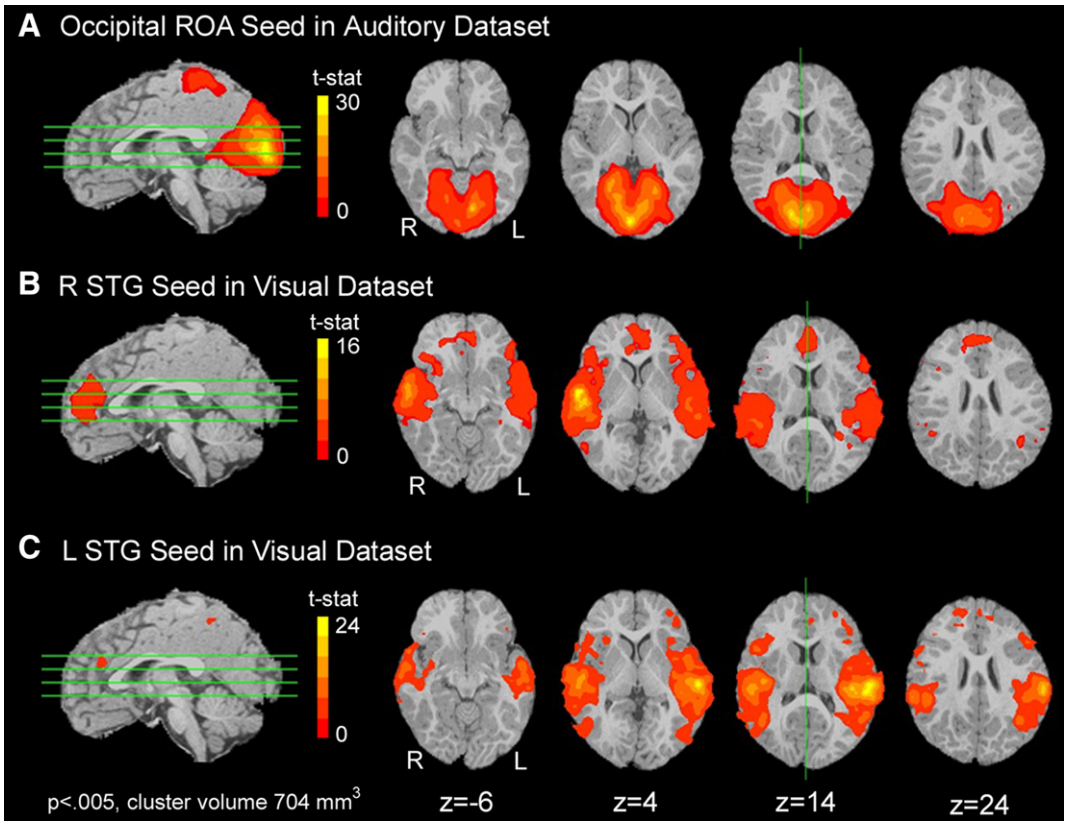

Fig. 4. Group functional connectivity maps. Maps are displayed on images from a single representative subject ($p<0.005$, corrected). Functional connectivity analyses were performed for three ROAs identified in the stimulus-evoked analyses: left STG, right STG, and occipital cortex. In order to identify stimulus-independent patterns of connectivity, the visual ROA was used as a seed region in the auditory datasets while two auditory ROAs were used as seed regions in the visual datasets. Axial coordinates (x, y, z) are given for each slice.

for the differential auditory response between conditions found in the current study.

Although the regions responsive to visual stimuli were similar to those seen during visual stimulation while awake with eyes open (e.g., primary visual cortex and surrounding extrastriate areas), the sign of the response was different. Specifically, visual cortex showed a pattern of BOLD signal decrease when presented with flashing light stimuli as compared to no stimulus presentation. Studies of the sedated infant (Martin et al., 1999; Morita et al., 2000; Yamada et al., 2000), sedated child (Altman and Bernal, 2001) and sleeping adult (Born et al., 2002) have also reported BOLD signal decrease in visual cortex in response to flashing lights. Furthermore, in unpublished pilot data from our lab, very similar regions showed negative BOLD signal in response to the same stimulus paradigm in two awake adults with their eyes closed (Supplementary information Fig. S3). Thus, BOLD signal decrease in response to visual stimuli is seen across multiple ages and behavioral states (sleep, sedation, or awake with eyes closed) with the common denominator being eyes closed. Although not yet completely understood, studies of awake adults resting with eyes closed reveal reduced levels of cerebral blood flow from both PET (Raichle et al., 2001) and ASL measurements (Uludag et al., 2004). In the current study, the children's eyes were closed the entire time and BOLD signal was decreased during periods of visual stimulation as compared to no stimulation. The reason for this decrease is speculative without information on changes in blood flow but could reflect inhibition of visual input when eyes are closed.

In addition to examining the neurofunctional response to external stimuli, the present study showed that sleep fMRI can be used to examine the internal, intrinsic organization of the brain in very young children. By examining spontaneous fluctuations in auditory-related regions (i.e., right and left STG) during the visual experiment, auditory functional networks that are independent of the stimulus-related activations were identified. For each auditory seed region (left or right STG/S), significant correlations with the contralateral superior temporal regions were found, in addition to numerous other regions in temporal, frontal, and parietal cortex (see Table 4). Interestingly, in this study, functional connectivity of the auditory system showed robust connections to higher order prefrontal regions while functional connectivity analyses of the visual system did not. Visual cortex, on the other hand, showed functional connectivity patterns with surrounding extrastriate and parietal areas. The differential functional connectivity patterns identified with auditory and visual seed regions provide evidence for dissociable networks that can be identified without presentation of a specific, external stimulus. Given our stimulus-evoked and stimulus-independent analyses, we suggest the auditory system is an ideal system with which to study fMRI response during sleep as it shows intrinsic, spontaneous functional connectivity to a number of higher order regions during sleep and discrimination between auditory stimulus types.

The majority of regions identified during stimulus-evoked analyses (either auditory or visual) were identified during the stimulus-independent fcMRI analyses; however, fcMRI analyses

revealed a greater extent and number of brain regions. This finding suggests that functional connectivity analyses allow for identification of whole networks while stimulus-evoked analyses show activation in portions of the network which are differentially engaged for the specific type of stimulus presentation. An exception is seen in the cerebellum, two occipital regions, and the putamen. Stimulus-evoked activations to tones and nonvocal sounds were seen in these regions but not in the functional connectivity analyses with left or right STG regions. Other stimulus-evoked and fcMRI studies have shown activation of the cerebellum during stimulus-evoked fMRI but not stimulus-independent, resting fcMRI analyses (Cordes et al., 2000). These findings suggest that certain regions which are active during stimulus-evoked analyses, such as the cerebellum, may not be part of a specific functional network, but rather may be engaged for processing auditory or other stimulus types when needed. This hypothesis is consistent with a proposed role of the cerebellum as a general purpose structure whose role is to predict and strategically prepare the necessary neural systems needed to perform a variety of different functions (Courchesne and Allen, 1997).

The use of sleep fMRI in the study of typical and atypical development poses several advantages over other methods of developmental cognitive neuroscience. First, fMRI allows for the identification of specific cortical and sub-cortical substrates with relatively good anatomical spatial resolution. Recording during sleep strongly minimizes artifacts or loss of participant data due to motion artifact. Second, sleep fMRI allows for a comparable state of eyes-closed passive perception across participants. Often studies of children and particularly those with developmental disorders are not only measuring stimulus specific effects but also those related to differences in anxiety, motivation, arousal state, or attention. When comparing typically with atypically developing children, differences in brain activations may be due to these confounds rather than the stimulus in question. Third, sleep fMRI allows for the study of stimulus-independent fluctuations in BOLD signal across different ages from infancy to adulthood which may provide valuable insight into the development of these and other functional networks. Further, our findings suggest stimulus-independent functional connectivity can reveal the functional organization of entire networks which may be missed by stimulus-evoked analyses alone. As shown in this study, fcMRI can identify regions involved in stimulus-evoked analyses without limiting findings to a specific type of stimulus presentation. This method can be applied to children with developmental disorders with known abnormalities of functional connectivity such as autism (Horwitz et al., 1988; Just et al., 2004; Villalobos et al., 2005). Of course, a limitation of sleep fMRI is that the neural response to certain stimuli during sleep is not always as predicted from the awake state. Furthermore, future research will need to address the question of how different sleep stages may affect different patterns of brain activations. It will also be important to determine how these differential BOLD responses during sleep relate to behavioral abilities in the awake child. Converging evidence from sleep fMRI and awake behavioral performance could enhance understanding of early functional brain organization.

Acknowledgments

The authors are grateful to the parents and children who participated in this study. We thank Dr. Cindy Carter for psychological testing, Vera Grindell, Anne Erickson, Grace Kim, Cindy Hsu, and Randy Wu for assistance with data collection, and Dr. Saygin and colleagues for sharing their sound stimuli. This work was supported by the National Institutes of Health grants RO1-NS-19855 and MH-36840 and a gift from the Donald C. and Elizabeth M. Dickinson Foundation awarded to E.C.

Appendix A. Supplementary data

Supplementary data associated with this article can be found, in the online version, at doi:10.1016/j.neuroimage.2007.08.005.

References

Altman, N.R., Bernal, B., 2001. Brain activation in sedated children: auditory and visual functional MR imaging. Radiology 221, 56–63.

Anderson, A.W., Marois, R., Colson, E.R., Peterson, B.S., Duncan, C.C., Ehrenkranz, R.A., Schneider, K.C., Gore, J.C., Ment, L.R., 2001. Neonatal auditory activation detected by functional magnetic resonance imaging. Magn. Reson. Imaging 19, 1–5.

Bartles, A., Zeki, S., 2005. Brain dynamics during natural viewing conditions – a new guide for mapping connectivity in vivo. NeuroImage 24, 339–349.

Bastuji, H., Perrin, F., Garcia-Larrea, L., 2002. Semantic analysis of auditory input during sleep: studies with event related potentials. Int. J. Psychophysiol. 46, 243–255.

Belin, P., Zatorre, R.J., Lafaille, P., Ahad, P., Pike, B., 2000. Voice-selective areas in human auditory cortex. Nature 403, 309–312.

Belin, P., Zatorre, R.J., Ahad, P., 2002. Human temporal-lobe response to vocal sounds. Brain Res. Cogn. Brain Res. 13, 17–26.

Biswal, B., Yetkin, F.Z., Haughton, V.M., Hyde, J.S., 1995. Functional connectivity in the motor cortex of resting human brain using echo-planar MRI. Magn. Reson. Med. 34, 537–541.

Born, P., Rostrup, E., Leth, H., Peitersen, B., Lou, H.C., 1996. Change of visually induced cortical activation patterns during development. Lancet 347, 543.

Born, A.P., Law, I., Lund, T.E., Rostrup, E., Hanson, L.G., Wildschiodtz, G., Lou, H.C., Paulson, O.B., 2002. Cortical deactivation induced by visual stimulation in human slow-wave sleep. NeuroImage 17, 1325–1335.

Carver, L.J., Dawson, G., Panagiotides, H., Meltzoff, A.N., Mcpartland, J., Gray, J., Munson, J., 2003. Age-related differences in neural correlates of face recognition during the toddler and preschool years. Dev. Psychobiol. 42, 148–159.

Cheour, M., Ceponiene, R., Leppanen, P., Alho, K., Kujala, T., Renlund, M., Fellman, V., Naatanen, R., 2002a. The auditory sensory memory trace decays rapidly in newborns. Scand. J. Psychol. 43, 33–39.

Cheour, M., Martynova, O., Naatanen, R., Erkkola, R., Sillanpaa, M., Kero, P., Raz, A., Kaipio, M.L., Hiltunen, J., Aaltonen, O., et al., 2002b. Speech sounds learned by sleeping newborns. Nature 415, 599–600.

Cordes, D., Haughton, V.M., Arfanakis, K., Wendt, G.J., Turski, P.A., Moritz, C.H., Quigley, M.A., Meyerand, M.E., 2000. Mapping functionally related regions of brain with functional connectivity MR imaging. AJNR Am. J. Neuroradiol. 21, 1636–1644.

Courchesne, E., Allen, G., 1997. Prediction and preparation, fundamental functions of the cerebellum. Learn. Mem. 4, 1–35.

Courchesne, E., Chisum, H., Townsend, J., Cowles, A., Covington, J., Egaas, B., Hinds, S., Press, G., 2000. Normal brain development and aging: quantitative analysis at in vivo MR imaging in healthy volunteers. Radiology 216, 672–682.

Cox, R.W., 1996. AFNI: software for analysis and visualization of functional magnetic resonance neuroimages. Comput. Biomed. Res. 29, 162–173.

Cummings, A., Ceponiene, R., Koyama, A., Saygin, A.P., Townsend, J., Dick, F., 2006. Auditory semantic networks for words and natural sounds. Brain Res. 1115, 92–107.

Czisch, M., Wetter, T.C., Kaufmann, C., Pollmacher, T., Holsboer, F., Auer, D.P., 2002. Altered processing of acoustic stimuli during sleep: reduced

auditory activation and visual deactivation detected by a combined fMRI/EEG study. NeuroImage 16, 251–258.
Czisch, M., Wehrle, R., Kaufmann, C., Wetter, T.C., Holsboer, F., Pollmacher, T., Auer, D.P., 2004. Functional MRI during sleep: BOLD signal decreases and their electrophysiological correlates. Eur. J. Neurosci. 20, 566–574.
Dehaene-Lambertz, G., Dehaene, S., Hertz-Pannier, L., 2002. Functional neuroimaging of speech perception in infants. Science 298, 2013–2015.
Fox, M.D., Snyder, A.Z., Vincent, J.L., Corbetta, M., Van Essen, D.C., Raichle, M.E., 2005. The human brain is intrinsically organized into dynamic, anticorrelated functional networks. Proc. Natl. Acad. Sci. U. S. A. 102, 9673–9678.
Fox, M.D., Corbetta, M., Snyder, A.Z., Vincent, J.L., Raichle, M.E., 2006. Spontaneous neuronal activity distinguishes human dorsal and ventral attention systems. Proc. Natl. Acad. Sci. U. S. A. 103, 10046–10051.
Fransson, P., 2005. Spontaneous low-frequency BOLD signal fluctuations: an fMRI investigation of the resting-state default mode of brain function hypothesis. Hum. Brain Mapp. 26, 15–29.
Friederici, A.D., 2006. The neural basis of language development and its impairment. Neuron 52, 941–952.
Fukunaga, M., Horovitz, S.G., Van Gelderen, P., De Zwart, J.A., Jansma, J.M., Ikonomidou, V.N., Chu, R., Deckers, R.H., Leopold, D.A., Duyn, J.H., 2006. Large-amplitude, spatially correlated fluctuations in BOLD fMRI signals during extended rest and early sleep stages. Magn. Reson. Imaging 24, 979–992.
Gaab, N., Gabrieli, J.D., Glover, G.H., 2006. Assessing the influence of scanner background noise on auditory processing. II. An fMRI study comparing auditory processing in the absence and presence of recorded scanner noise using a sparse design. Hum. Brain Mapp. 28, 703–720.
Greicius, M.D., Krasnow, B., Reiss, A.L., Menon, V., 2003. Functional connectivity in the resting brain: a network analysis of the default mode hypothesis. Proc. Natl. Acad. Sci. U. S. A. 100, 253–258.
Horwitz, B., Rumsey, J.M., Grady, C.L., Rapoport, S.I., 1988. The cerebral metabolic landscape in autism. Intercorrelations of regional glucose utilization. Arch. Neurol. 45, 749–755.
Huttenlocher, P., 2002. Neural Plasticity: The Effects of Environment on the Development of Cerebral Cortex. Harvard Univ. Press, Cambridge, MA.
Huttenlocher, P.R., Dabholkar, A.S., 1997. Regional differences in synaptogenesis in human cerebral cortex. J. Comp. Neurol. 387, 167–178.
Jancke, L., Shah, N.J., Posse, S., Grosse-Ryuken, M., Muller-Gartner, H.W., 1998. Intensity coding of auditory stimuli: an fMRI study. Neuropsychologia 36, 875–883.
Just, M.A., Cherkassky, V.L., Keller, T.A., Minshew, N.J., 2004. Cortical activation and synchronization during sentence comprehension in high-functioning autism: evidence of underconnectivity. Brain 127, 1811–1821.
Langers, D.R., Van Dijk, P., Schoenmaker, E.S., Backes, W.H., 2007. fMRI activation in relation to sound intensity and loudness. NeuroImage 35, 709–718.
Marcar, V.L., Strassle, A.E., Loenneker, T., Schwarz, U., Martin, E., 2004. The influence of cortical maturation on the BOLD response: an fMRI study of visual cortex in children. Pediatr. Res. 56, 967–974.
Martin, E., Joeri, P., Loenneker, T., Ekatodramis, D., Vitacco, D., Hennig, J., Marcar, V.L., 1999. Visual processing in infants and children studied using functional MRI. Pediatr. Res. 46, 135–140.
Martynova, O., Kirjavainen, J., Cheour, M., 2003. Mismatch negativity and late discriminative negativity in sleeping human newborns. Neurosci. Lett. 340, 75–78.
Morita, T., Kochiyama, T., Yamada, H., Konishi, Y., Yonekura, Y., Matsumura, M., Sadato, N., 2000. Difference in the metabolic response to photic stimulation of the lateral geniculate nucleus and the primary visual cortex of infants: a fMRI study. Neurosci. Res. 38, 63–70.
Nir, Y., Hasson, U., Levy, I., Yeshurun, Y., Malach, R., 2006. Widespread functional connectivity and fMRI fluctuations in human visual cortex in the absence of visual stimulation. NeuroImage 30, 1313–1324.
Pena, M., Maki, A., Kovacic, D., Dehaene-Lambertz, G., Koizumi, H., Bouquet, F., Mehler, J., 2003. Sounds and silence: an optical topography study of language recognition at birth. Proc. Natl. Acad. Sci. U. S. A. 100, 11702–11705.
Perrin, F., Garcia-Larrea, L., Mauguiere, F., Bastuji, H., 1999. A differential brain response to the subject's own name persists during sleep. Clin. Neurophysiol. 110, 2153–2164.
Perrin, F., Bastuji, H., Garcia-Larrea, L., 2002. Detection of verbal discordances during sleep. NeuroReport 13, 1345–1349.
Portas, C.M., Krakow, K., Allen, P., Josephs, O., Armony, J.L., Frith, C.D., 2000. Auditory processing across the sleep–wake cycle: simultaneous EEG and fMRI monitoring in humans. Neuron 28, 991–999.
Raichle, M.E., Macleod, A.M., Snyder, A.Z., Powers, W.J., Gusnard, D.A., Shulman, G.L., 2001. A default mode of brain function. Proc. Natl. Acad. Sci. U. S. A. 98, 676–682.
Redcay, E., Haist, F., Courchesne, E., in press. Functional neuroimaging of speech perception during a pivotal period of language acquisition. Developmental Science.
Saygin, A.P., Dick, F., Wilson, S.M., Dronkers, N.F., Bates, E., 2003. Neural resources for processing language and environmental sounds: evidence from aphasia. Brain 126, 928–945.
Saygin, A.P., Dick, F., Bates, E., 2005. An on-line task for contrasting auditory processing in the verbal and nonverbal domains and norms for younger and older adults. Behav. Res. Methods 37, 99–110.
Seeley, W.W., Menon, V., Schatzberg, A.F., Keller, J., Glover, G.H., Kenna, H., Reiss, A.L., Greicius, M.D., 2007. Dissociable intrinsic connectivity networks for salience processing and executive control. J. Neurosci. 27, 2349–2356.
Sie, L.T.L., Rombouts, S.A., Valk, I.J., Hart, A.A., Scheltens, P., Van Der Knaap, M.S., 2001. Functional MRI of visual cortex in sedated 18-month-old infants with or without periventricular leukomalacia. Dev. Med. Child Neurol. 43, 486–490.
Souweidane, M.M., Kim, K.H., Mcdowall, R., Ruge, M.I., Lis, E., Krol, G., Hirsch, J., 1999. Brain mapping in sedated infants and young children with passive-functional magnetic resonance imaging. Pediatr. Neurosurg. 30, 86–92.
Talairach, J., Tournoux, P., 1988. Co-planar Stereotaxic Atlas of the Human Brain. Thieme Medical Publishers, New York.
Tanaka, H., Fujita, N., Takanashi, M., Hirabuki, N., Yoshimura, H., Abe, K., Nakamura, H., 2003. Effect of stage 1 sleep on auditory cortex during pure tone stimulation: evaluation by functional magnetic resonance imaging with simultaneous EEG monitoring. AJNR Am. J. Neuroradiol. 24, 1982–1988.
Uludag, K., Dubowitz, D.J., Yoder, E.J., Restom, K., Liu, T.T., Buxton, R.B., 2004. Coupling of cerebral blood flow and oxygen consumption during physiological activation and deactivation measured with fMRI. NeuroImage 23, 148–155.
Villalobos, M.E., Mizuno, A., Dahl, B.C., Kemmotsu, N., Muller, R.-A., 2005. Reduced functional connectivity between V1 and inferior frontal cortex associated with visuomotor performance in autism. NeuroImage 25, 916–925.
Vincent, J.L., Snyder, A.Z., Fox, M.D., Shannon, B.J., Andrews, J.R., Raichle, M.E., Buckner, R.L., 2006. Coherent spontaneous activity identifies a hippocampal–parietal memory network. J. Neurophysiol. 96, 3517–3531.
Wehrle, R., Kaufmann, C., Wetter, T.C., Holsboer, F., Auer, D.P., Pollmacher, T., Czisch, M., 2007. Functional microstates within human REM sleep: first evidence from fMRI of a thalamocortical network specific for phasic REM periods. Eur. J. Neurosci. 25, 863–871.
Wilke, M., Holland, S.K., Ball Jr., W.S., 2003. Language processing during natural sleep in a 6-year-old boy, as assessed with functional MR imaging. AJNR Am. J. Neuroradiol. 24, 42–44.
Yamada, H., Sadato, N., Konishi, Y., Muramoto, S., Kimura, K., Tanaka, M., Yonekura, Y., Ishii, Y., Itoh, H., 2000. A milestone for normal development of the infantile brain detected by functional MRI. Neurology 55, 218–223.